Postprint of: Mikhasev G., Botogova M., Eremeev V., Anti-plane waves in an elastic thin strip with surface energy, PHILOSOPHICAL TRANSACTIONS OF THE ROYAL SOCIETY A-MATHEMATICAL PHYSICAL AND ENGINEERING SCIENCES Vol. 380, No 2231 (2022), pp.1-15, DOI: 10.1098/rsta.2021.0373

Anti-plane waves in an elastic thin strip with surface energy

G. I. Mikhasev[1], M. G. Botogova[1] and V. A. Eremeyev[2,3]

[1]Faculty of Mechanics and Mathematics, Belarusian State University, Nezavisimosty Ave. 4, 220030 Minsk, Belarus
[2]Department of Civil and Environmental Engineering and Architecture (DICAAR), University of Cagliari, Via Marengo 2, 09123 Cagliari, Italy
[3]Faculty of Civil and Environmental Engineering, Gdańsk University of Technology, ul. Gabriela Narutowicza 11/12, 80-233 Gdańsk, Poland

Subject Areas:
mechanical engineering, nanotechnology, structural engineering

Keywords:
surface elasticity, anti-plane waves, dispersion relations

Author for correspondence:
V. A. Eremeyev
e-mail: eremeyev.victor@gmail.com

We consider anti-plane motions of an elastic plate taking into account surface energy within the linear Gurtin–Murdoch surface elasticity. Two boundary-value problems are considered that describe complete shear dynamics of a plate with free faces or with free and clamped faces, respectively. These problems correspond to anti-plane dynamics of an elastic film perfectly or non-perfectly attached to a rigid substrate. Detailed analysis of dispersion relations is provided. In particular, the influence of the ratio of a plate thickness to characteristic length on the dispersion curves is analysed.

This article is part of the theme issue 'Wave generation and transmission in multi-scale complex media and structured metamaterials (part 1)'.

1. Introduction

Recent advances in nanotechnologies result in essential extension of applications of continuum mechanics and mechanics of structures towards modelling of material behaviour at small scales. Among various approaches used at micro- and nanoscale, it is worth mentioning the surface elasticity approach almost based on the Gurtin–Murdoch [1,2] and Steigmann–Ogden [3,4] models, see also [5–10]. Within this approach in addition to constitutive relations in the bulk, we introduce a surface energy density and surface stresses. From the physical point of view, surface elasticity models describe

coupled deformations of an elastic solid body with, perfectly attached to its surface, an elastic membrane or shell. The existence of a surface energy leads to the possibility to properly describe some phenomena such as various size-effects observed at the nanoscale [6,10].

From the mathematical point of view, related boundary-value problems (BVPs) include classic equation of motion and non-classic boundary conditions. Let us note that discussed non-classic boundary conditions are similar or even the same as derived for so-called stiff interfaces studied by Benveniste and Miloh [11,12], Mishuris *et al.* [13–15], or to the case of so-called hard-skins in plate theory [16], see also brief discussions in [17,18]. The surface elasticity approach is also closely related to surface/interface localization phenomena, models of media with thin coatings and non-local continua [19–24]. In particular, surface elasticity deeply correlates to Mindlin's strain gradient elasticity [25], e.g. [26], where straightforward comparison of the Mindlin–Toupin strain gradient elasticity with the Gurtin–Murdoch model was provided. This approach has an origin in the work by Korteweg [27] in the field of molecular capillarity. The Gurtin–Murdoch model could be also introduced as a continuum limit of lattice dynamics [28] if a certain scaling law was assumed.

Recently, surface elasticity models were widely used for the analysis of nanostructured materials, e.g. [6,8,10] and the references therein. It was shown that effective properties of nanostructured materials could essentially depend on the surface properties [6,8,29,30]. The presence of surface stresses may significantly change the behaviour of stress and displacement fields in the vicinity of geometrical singularities such as crack tips [18,31]. In addition to modification of effective properties of nanocomposite materials and essential changes in solution of corresponding BVPs, the surface elasticity approach results in new wave phenomena such as an appearance of anti-plane surface waves in media with surface energetics [32]. This phenomenon is similar to Love waves in an elastic half-space with a coating of finite thickness [33]. Nowadays, it is clear that surface elasticity may essentially change a picture of surface waves, e.g. [17,34–39] and the references therein. Characteristics of the propagation of anti-plane surface waves could be used for determination of surface elastic moduli [40–42].

Let us note that within the Gurtin–Murdoch model we face two length-scale parameters that are static and dynamic ones. The static length-scale parameter ℓ_s could be defined as a ratio of a surface shear modulus μ_s to a shear modulus μ in the bulk, $\ell_s = \mu_s/\mu$, whereas the dynamic length-scale parameter ℓ_d is defined as the ratio of a surface mass density ρ_s to a mass density in the bulk ρ, $\ell_d = \rho_s/\rho$. Obviously, for multiple surfaces or interfaces with different properties, we get more such parameters. These parameters bring a possibility to capture some size-effects, when a size of an object under consideration is close to one of these parameters. Considering in addition the roughness of a surface or interface, we get another length-scale parameter related to a magnitude of roughness [39,43,44]. So a proper description of solids with surface energetics constitutes a class of problems of multi-scale mechanics that requires additional attention to analysis of strain/stress localization.

In this paper, we consider anti-plane waves in an elastic plate endowed with surface stresses on at least one face. For this problem, we have at least three characteristic lengths such as ℓ_s, ℓ_d and thickness of the plate h. The paper is organized as follows. First, we briefly recall the statement of the problem using the linear Gurtin–Murdoch model for anti-plane shear in §2. Considering harmonic stationary solutions, in §3, we derive dispersion relations for a plate with free-clamped and free-free faces. Here, we consider two classes of solutions called transversally exponential (TE) and transversally harmonic (TH). TE solutions are similar to ones in the case of half-space, whereas TH ones are similar but not the same as Lamb waves. Finally, in order to underline an influence of finite thickness on the phase velocity, in §4, we present some examples of dispersion curves. It was shown that for thick enough plates a TE solution reduces to the case of an elastic half-space, whereas for a relatively thin plate we observe more complex behaviour. In other words, depending on the plate thickness and the wavelength we have some localized surface waves propagating along plate free faces.

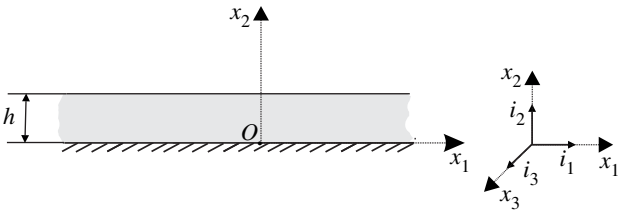

Figure 1. Infinite elastic plate-like domain and used Cartesian coordinate system.

2. Anti-plane deformations within linear Gurtin–Murdoch surface elasticity

Let us consider a three-dimensional elastic plate-like body of thickness h occupying a three-dimensional domain $\mathcal{D} = \{-\infty < x_1 < +\infty, 0 \le x_2 \le h, -\infty < x_3 < +\infty\}$, where x_k and $\mathbf{i}_k$, $k = 1, 2, 3$, are Cartesian coordinates and related unit base vectors, see figure 1. For anti-plane deformations, the vector of displacement $\mathbf{u}$ takes a simple form, e.g. [33],

$$\mathbf{u} = \mathbf{u}(x_1, x_2, x_3, t) = u(x_1, x_2, t)\mathbf{i}_3, \tag{2.1}$$

where t is time. In the following, we consider a homogeneous isotropic medium. Using Hooke's Law for anti-plane shear we get

$$\left.\begin{aligned} &\boldsymbol{\sigma} = 2\mu\boldsymbol{\varepsilon} = \sigma_{13}(\mathbf{i}_1 \otimes \mathbf{i}_3 + \mathbf{i}_3 \otimes \mathbf{i}_1) + \sigma_{23}(\mathbf{i}_2 \otimes \mathbf{i}_3 + \mathbf{i}_3 \otimes \mathbf{i}_2) \\ \text{and} \quad &\sigma_{13} = 2\mu\varepsilon_{13}, \quad \sigma_{23} = 2\mu\varepsilon_{23}, \end{aligned}\right\} \tag{2.2}$$

where $\boldsymbol{\sigma}$ and $\boldsymbol{\varepsilon}$ are the stress and strain tensors, respectively and μ is a constant shear modulus. For (2.1), the strain tensor is given by the formulae

$$\left.\begin{aligned} &\boldsymbol{\varepsilon} = \varepsilon_{13}(\mathbf{i}_1 \otimes \mathbf{i}_3 + \mathbf{i}_3 \otimes \mathbf{i}_1) + \varepsilon_{23}(\mathbf{i}_2 \otimes \mathbf{i}_3 + \mathbf{i}_3 \otimes \mathbf{i}_2) \\ \text{and} \quad &\varepsilon_{13} = \frac{1}{2}\frac{\partial u}{\partial x_1}, \quad \varepsilon_{23} = \frac{1}{2}\frac{\partial u}{\partial x_2}. \end{aligned}\right\} \tag{2.3}$$

Hereinafter $\otimes$ stands for the dyadic product.

As a result, the equation of motion in $\mathcal{D}$ takes the form of the wave equation [33]

$$\mu\left(\frac{\partial^2 u}{\partial x_1^2} + \frac{\partial^2 u}{\partial x_2^2}\right) = \rho\frac{\partial^2 u}{\partial t^2}, \tag{2.4}$$

where ρ is a mass density in the bulk.

In what follows, we consider two BVPs. On the free boundary $x_2 = h$ surface stresses are assumed that are described within the Gurtin–Murdoch model of surface elasticity [1,2]. On the boundary $x_2 = 0$, we consider two types of boundary conditions

(1) clamping in the x_3 – direction.
(2) the presence of surface stresses as on the face $x_2 = h$.

We call these BVPs *Problem I* and *Problem II*, respectively. Problem I describes shear of a thin film perfectly attached to a rigid substrate, whereas Problem II model describes anti-plane shear of a free suspended or thin film debonded from a substrate. So we have the following boundary conditions:

Problem I

$$\mu\frac{\partial u}{\partial x_2} = \mu_{sh}\frac{\partial^2 u}{\partial x_1^2} - \rho_{sh}\frac{\partial^2 u}{\partial t^2} \quad \text{at } x_2 = h \tag{2.5}$$

and

$$u = 0 \quad \text{at } x_2 = 0. \tag{2.6}$$

Problem II

$$\mu \frac{\partial u}{\partial x_2} = \mu_{sh} \frac{\partial^2 u}{\partial x_1^2} - \rho_{sh} \frac{\partial^2 u}{\partial t^2} \quad \text{at } x_2 = h \tag{2.7}$$

and

$$-\mu \frac{\partial u}{\partial x_2} = \mu_{s0} \frac{\partial^2 u}{\partial x_1^2} - \rho_{s0} \frac{\partial^2 u}{\partial t^2} \quad \text{at } x_2 = 0, \tag{2.8}$$

where μ_{s0}, μ_{sh} are surface shear moduli and ρ_{s0}, ρ_{sh} are surface mass densities for the planes $x_2 = 0, h$, respectively, introduced in [2]. For example, the following material parameters of iron were used in [2,6]: $\mu_{sh} = 2.5\,\text{N m}^{-1}$, $\mu = 70\,\text{GPa}$, $\rho_{sh} = 7 \times 10^{-6}\,\text{kg m}^{-2}$, $\rho = 7 \times 10^3\,\text{kg m}^{-3}$. Here, $\ell_{dh} = = \rho_{sh}/\rho = 10^{-9}\,\text{m}$, $c_T = \sqrt{\mu/\rho} = 3162.27\,\text{m s}^{-1}$, $c_{sh} = \sqrt{\mu_{sh}/\rho_{sh}} = 597.61\,\text{m s}^{-1}$. Here, we have a difference in length-scale parameters as $\ell_d = 10^{-9}$ m and $\ell_s = 0.36 \times 10^{-10}$ m. For derivation of dynamic boundary conditions (2.5) and (2.8), we refer to [32]. Note that if $\mu_{s0} = \rho_{s0} = 0$ or/and $\mu_{sh} = \rho_{sh} = 0$, then the surface shear stresses and inertia on a lower or/and upper surface(s) are ignored. In this case, a boundary condition for an anti-plane wave on a correspondent surface becomes classical, $\partial u/\partial x_2 = 0$.

3. Dispersion equations

An analysis of the wave equation (2.4) indicates the existence of two regimes of anti-plane stationary waves: (a) waves decaying exponentially from the upper and lower surfaces and (b) waves with harmonic behaviour in the transverse direction. In what follows, these two types of running waves will be called the TE and TH regimes of anti-plane waves, respectively.

Considering the TE regime of anti-plane waves, we are looking for a solution of equation (2.4) in the form

$$u = U e^{i(kx_1 - \omega t)} [a_1\, e^{\alpha(x_2 - h)} + a_2\, e^{-\alpha x_2}], \quad i = \sqrt{-1}, \tag{3.1}$$

where U is a constant amplitude, a_1, a_2 are integration constants that have to be defined from boundary conditions, k is a wavenumber and ω is the circular frequency. A positive parameter α characterizes an attenuation rate of the wave amplitude. After substitution of (3.1) into (2.4), we find α as follows:

$$\alpha = |k| \sqrt{1 - \frac{c^2}{c_T^2}}, \tag{3.2}$$

where $c = \omega/k$ is the phase velocity, and $c_T = \sqrt{\mu/\rho}$ is the shear wave speed in an elastic medium. Here, $c < c_T$ as for a half-space with surface stresses [32].

For TH anti-plane waves, a solution of equation (2.4) is sought in the form

$$u = U\, e^{i(kx_1 - \omega t)}\, (b_1 \sin \lambda x_2 + b_2 \cos \lambda x_2), \tag{3.3}$$

with b_1, b_2 being constants, and

$$\lambda = |k| \sqrt{\frac{c^2}{c_T^2} - 1} > 0. \tag{3.4}$$

So for the harmonic solution we have $c > c_T$.

TE and TH regimes correspond to real and imaginary roots of the characteristic equations related to (2.4).

(a) Solution of Problem I

(i) TE regime of anti-plane waves

Substituting (3.1) into the boundary conditions (2.5) and (2.6), we arrive at the following two equations with respect to a_1 and a_2:

$$(\mu\alpha + \mu_{sh}k^2 - \rho_{sh}\omega^2)a_1 + (\mu_{sh}k^2 - \rho_{sh}\omega^2 - \mu\alpha)\,\mathrm{e}^{-\alpha h}a_2 = 0 \tag{3.5}$$

and

$$\mathrm{e}^{-\alpha h}a_1 + a_2 = 0. \tag{3.6}$$

Using (3.2) with the latter equations, we get the dispersion equation written in the dimensionless form as follows:

$$\frac{1}{|k|\ell_{dh}}\sqrt{1-\frac{c^2}{c_T^2}} + \frac{c_{sh}^2}{c_T^2} - \frac{c^2}{c_T^2} - \exp\left[-2|k|h\sqrt{1-\frac{c^2}{c_T^2}}\right]\left(\frac{c_{sh}^2}{c_T^2} - \frac{c^2}{c_T^2} - \frac{1}{|k|\ell_{dh}}\sqrt{1-\frac{c^2}{c_T^2}}\right) = 0, \tag{3.7}$$

where $\ell_{dh} = \rho_{sh}/\rho$ is the dynamic length-scale parameter of the Gurtin–Murdoch model, and $c_{sh} = \sqrt{\mu_{sh}/\rho_{sh}}$ is the shear wave speed related to the elastic film attached to the face $x_2 = h$.

Considering a fixed value of k and $c < c_T$, we can prove that at $h \to +\infty$ equation (3.7) degenerates into the dispersion equation for a half-space

$$\frac{1}{|k|\ell_{dh}}\sqrt{1-\frac{c^2}{c_T^2}} + \frac{c_{sh}^2}{c_T^2} - \frac{c^2}{c_T^2} = 0, \tag{3.8}$$

which was studied in [32] in more detail. For a half-space with surface stresses, there is a unique solution of (3.8) in the range

$$c_{sh} < c < c_T. \tag{3.9}$$

So an anti-plane surface wave exists only if $c_{sh} < c_T$. Instead, for a plate of finite thickness, equation (3.7) has two solutions corresponding to the TE regime of anti-plane waves. The first one is trivial: $c = c_T$. This root does not correspond to any wave. Indeed, this solution corresponds to the multiple zero root of the characteristic equation related to (2.4). So u has the following form:

$$u = U\,\mathrm{e}^{i(kx_1 - \omega t)}(c_1 + c_2x_2),$$

with two unknown constants c_1 and c_2. As $u = 0$ at $x_2 = 0$, we have $c_1 = 0$. From (2.5), it follows that $c_2 = 0$. So $u = 0$ and in what follows we exclude this root. The second, non-trivial, solution represents a dispersive wave. In figure 2, the dimensionless velocity $v = c/c_T$ is shown as a function of dimensionless parameters $\delta_1 = |k|\rho_{sh}/\rho$ and $\delta_2 = |k|h$ for different values of $v_s = c_{sh}/c_T = 0.2, 0.4, 0.6$. It is seen that c increases with the increase of v_s. In addition, $c \to c_T$ at $h \to 0$ or/and if the wavelength $2\pi/|k|$ increases.

Let us note that without surface enhancement a TE solution does not exist. Indeed, if ρ_{sh} and μ_{sh} vanish, from (3.5) and (3.6), we get the equation

$$\mu\alpha(1 + \mathrm{e}^{-2\alpha h}) = 0,$$

which has only one solution $\alpha = 0$, that is $c = c_T$.

(ii) TH regime of anti-plane waves

Substituting (3.3) into (2.5) and (2.6), we get $b_2 = 0$. So u takes a sinusoidal in x_2-direction form

$$u = U\mathrm{e}^{i(kx_1 - \omega t)}\sin\lambda x_2$$

with new constant U. As a result, we came to the following dispersion equation:

$$\tan\left(h|k|\sqrt{\frac{c^2}{c_T^2} - 1}\right) = \frac{\sqrt{(c^2/c_T^2) - 1}}{|k|\ell_d((c^2/c_T^2) - (c_{sh}^2/c_T^2))}. \tag{3.10}$$

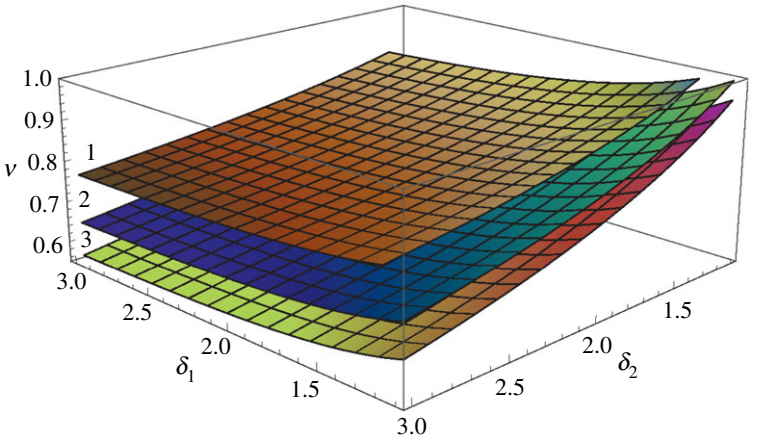

Figure 2. The dispersion surfaces $v = v(\delta_1, \delta_2)$ for an elastic plate with free and fixed faces for different values of a relative velocity $v_s = c_{sh}/c_T = 0.2, 0.4, 0.6$, labelled by 3, 2, 1 (lower, middle and upper surfaces), respectively. (Online version in colour.)

Obviously, in addition to the trivial root $c = c_T$, which should be excluded, for any fixed k, this equation has an infinite number of roots, $c = c_n(k)$. For $n \gg 1$, these roots could be represented by the following asymptotic relation:

$$c_n = c_T \sqrt{1 + \frac{1}{k^2 h^2}\left[\pi n + \frac{h}{\ell_d \pi n} - \frac{(3\ell_d + h)h^2}{3(\ell_d \pi n)^3}\right]^2}. \tag{3.11}$$

Let us again consider a problem without surface stresses. Then (2.5) results in a simple dispersion relation $\cos(h|k|\sqrt{(c^2/c_T^2) - 1}) = 0$, which has the series of roots

$$c_j = c_T \sqrt{1 + \frac{1}{k^2 h^2}\left(\pi j + \frac{\pi}{2}\right)^2}, \quad j = 0, 1, 2, \ldots \tag{3.12}$$

Thus, Problem I admits a solution in the form of anti-plane waves harmonically varying in the thickness direction.

(b) Solution of Problem II

(i) TE regime of anti-plane waves

Let us now consider anti-plane waves in a plate with free faces. Now instead of (3.6), we have

$$(\mu\alpha - \mu_{s0}k^2 + \rho_{s0}\omega^2)\,\mathrm{e}^{-\alpha h} a_1 + (-\mu\alpha - \mu_{s0}k^2 + \rho_{s0}\omega^2)\,a_2 = 0. \tag{3.13}$$

With (3.2) equations (3.5) and (3.13) results in the following dimensionless dispersion equation:

$$\left(\frac{1}{|k|\ell_{dh}}\sqrt{1 - \frac{c^2}{c_T^2}} + \frac{c_{sh}^2}{c_T^2} - \frac{c^2}{c_T^2}\right)\left(-\frac{1}{|k|\ell_{d0}}\sqrt{1 - \frac{c^2}{c_T^2}} - \frac{c_{s0}^2}{c_T^2} + \frac{c^2}{c_T^2}\right)$$
$$-\left(\frac{1}{|k|\ell_{dh}}\sqrt{1 - \frac{c^2}{c_T^2}} - \frac{c_{sh}^2}{c_T^2} + \frac{c^2}{c_T^2}\right)\left(-\frac{1}{|k|\ell_{d0}}\sqrt{1 - \frac{c^2}{c_T^2}} + \frac{c_{s0}^2}{c_T^2} - \frac{c^2}{c_T^2}\right)\exp\left[-2|k|h\sqrt{1 - \frac{c^2}{c_T^2}}\right] = 0, \tag{3.14}$$

where $\ell_{d0} = \rho_{s0}/\rho$ is the second dynamic length-scale parameter related to the face $x_2 = 0$. This equation also has a constant solution $c = c_T$. As in the previous case, we exclude it from consideration. In addition to it, there are another two roots of (3.14), in general. For fixed k and at $h \to \infty$, equation (3.14) degenerates into two dispersion relations similar to (3.8) as in the previous

case. This situation describes a propagation of two surface waves localized in the vicinity of free faces.

Let us consider one free surface without surface stresses. For example, we assume that $\rho_{s0} = \mu_{s0} = 0$, i.e. the surface effects on the lower surface are ignored. Then the dispersion equation (3.14) takes the form

$$\frac{1}{|k|\ell_{dh}}\sqrt{1-\frac{c^2}{c_T^2}}+\frac{c_{sh}^2}{c_T^2}-\frac{c^2}{c_T^2}-\left(\frac{1}{|k|\ell_{dh}}\sqrt{1-\frac{c^2}{c_T^2}}-\frac{c_{sh}^2}{c_T^2}+\frac{c^2}{c_T^2}\right)\exp\left[-2|k|h\sqrt{1-\frac{c^2}{c_T^2}}\right]=0. \tag{3.15}$$

Contrary to equation (3.14), this equation has only one root corresponding to an anti-plane wave.

Finally, if we neglect surface stresses on both faces, similarly to Problem I, we can show that Problem II has no solution in the form of anti-plane waves.

(ii) TH regime of anti-plane waves

To study TH waves in Problem II, we substitute (3.3) into (2.7) and (2.8). As a result, we arrive at a relation between b_1 and b_2

$$b_2 = \frac{\sqrt{(c^2/c_T^2)-1}}{k\ell_{d0}((c_{s0}^2/c_T^2)-(c^2/c_T^2))}b_1, \tag{3.16}$$

and come to the following dispersion equation:

$$\tan\left(h|k|\sqrt{\frac{c^2}{c_T^2}-1}\right)=\frac{|k|\sqrt{(c^2/c_T^2)-1}[\ell_{d0}((c_{s0}^2/c_T^2)-(c^2/c_T^2))+\ell_{dh}((c_{sh}^2/c_T^2)-(c^2/c_T^2))]}{(c^2/c_T^2)-1-k^2\ell_{d0}\ell_{dh}((c_{s0}^2/c_T^2)-(c^2/c_T^2))((c_{sh}^2/c_T^2)-(c^2/c_T^2))}. \tag{3.17}$$

Again, we exclude here the trivial root $c = c_T$. Other roots form an infinite series and grow up together with the mode number n for any fixed wave parameter k. For $n \gg 1$, they could be approximated by the following asymptotic relation:

$$c_n = c_T\sqrt{1+\frac{1}{(kh)^2}\left\{\pi n+\frac{h(\ell_{d0}+\ell_{dh})}{\pi n\ell_{d0}\ell_{dh}}-\frac{h^2(\ell_{d0}+\ell_{dh})^2[3\ell_{d0}\ell_{dh}+h(\ell_{d0}+\ell_{dh})]}{3(\pi n\ell_{d0}\ell_{dh})^3}\right\}^2}. \tag{3.18}$$

As above for the TE regime, simplified dispersion equations relating to cases where surface effects are not taken into account on one or both surfaces could be easily derived from equation (3.17). For brevity, they are not given here.

In what follows, we discuss the derived dispersion relations and corresponding dispersion curves in more detail.

4. Dispersion curves

(a) Problem I. TE regime

Dispersion curves for anti-plane TE waves are given in figures 3 and 4. In figure 3, dispersion relations are shown for relatively thin plates. Here, we present a relative velocity $v = c/c_T$ versus a dimensionless wavenumber $\bar{k} = k\ell_d$ for various values of dimensionless thickness $\bar{h} = h/\ell_d$, $\ell_d \equiv \ell_{dh}$. Curves 1, 2 and 3 correspond to $\bar{h} = 0.1, 1$ and 5, respectively. The red dashed curve (HS-curve) relates to the case of an elastic half-space ($h \to \infty$), whereas two horizontal dashed black lines are given by equations $c = c_T$ and $c = c_s \equiv c_{sh}$, $c_s < c_T$. For calculation, we also assumed that $c_s = 0.25\ c_T$. We see that for any plate thickness dispersion curves lie between line $c/c_T = 1$ and the HS-curve. All curves almost coincide with each other at $\bar{k} \to \infty$, i.e. for short-length waves. Instead, for long-length waves ($\bar{k} \to 0$), we see an essential difference. For a plate of finite thickness dispersion curves begin at line $c = c_T$ for a non-zero value of $\bar{k} = k^*$. So there is a range $\bar{k} \in (0, k^*)$ when waves related to the TE regime do not exist, whereas for a half-space the dispersion curve begins at the point $(0, c_T)$ with horizontal tangent.

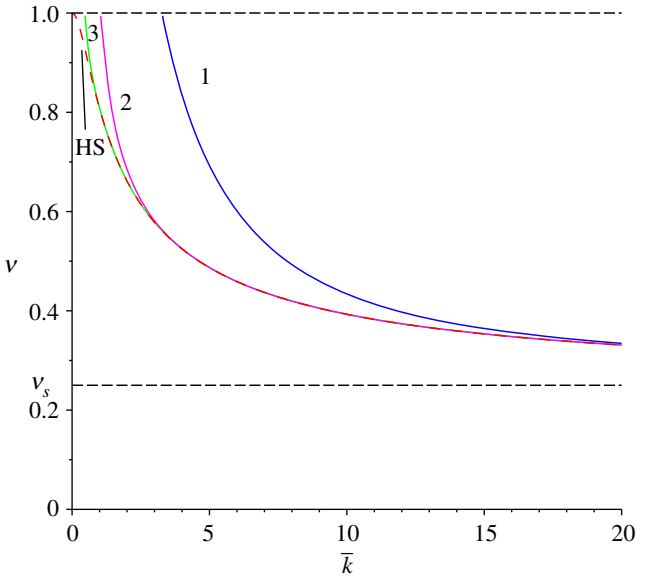

Figure 3. Problem I (TE regime). Dimensionless phase velocity $v = c/c_T$ versus wavenumber $\bar{k} = k\ell_d$. Curves 1, 2 and 3 correspond to thickness $h = 0.1\ell_d$, ℓ_d and $5\ell_d$, respectively. The red dashed curve marked by HS describes the case of a half-space ($h \to \infty$). Here, $c_s = 0.25c_T$, $v_s = c_s/c_T$. (Online version in colour.)

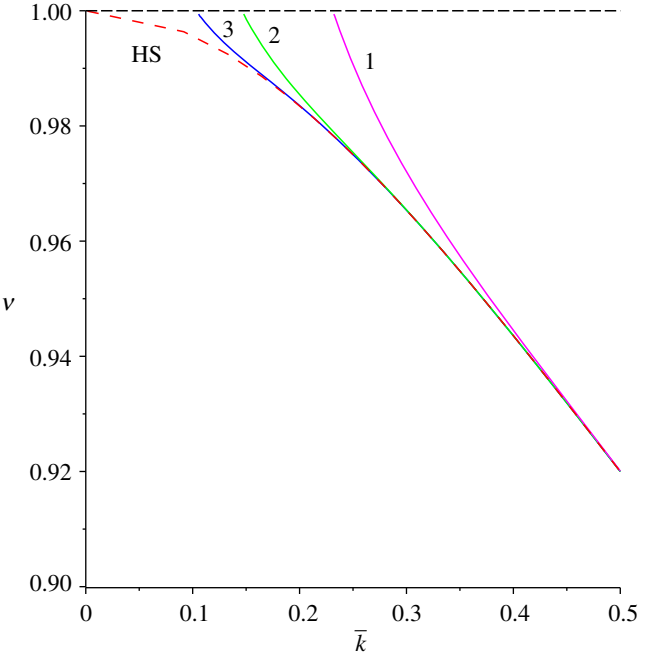

Figure 4. Problem I (TE regime). Dimensionless phase velocity $v = c/c_T$ versus wavenumber $\bar{k} = k\ell_d$. Curves 1, 2 and 3 correspond to thickness $h = 20\ell_d$, $50\ell_d$ and $100\ell_d$, respectively. Other data as in figure 3. (Online version in colour.)

In figure 4, dispersion curves are given for relatively thick plates. Here, the line $c = c_s$ is not shown and $\bar{h} = 20, 50, 100$, the corresponding curves are marked by 1, 2 and 3, respectively. The further analysis of figures 3 and 4 shows that the shorter the wavelength, the closer the dispersion curve to the curve for a half-space. In other words, clamped face could be useful

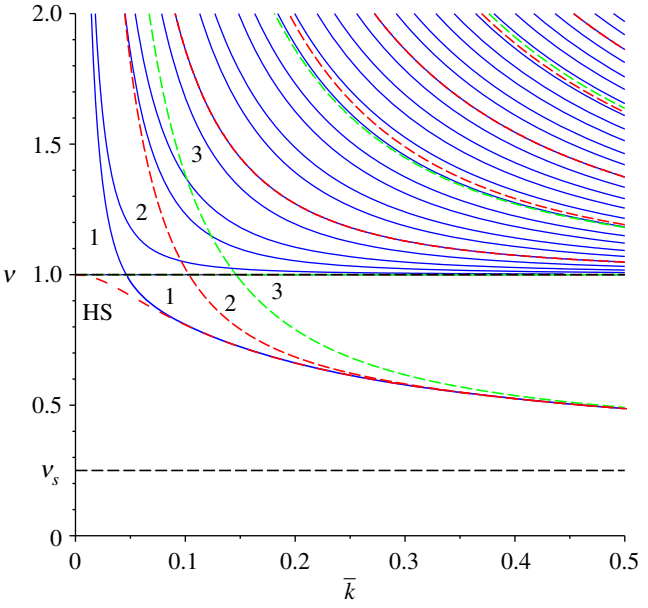

Figure 5. Problem I (TH and TE regimes). Dimensionless phase velocity $v = c/c_T$ versus wave number $\bar{k} = k\ell_d$. For the TH regime, we have three series of curves 1, 2 and 3 shown as solid blue, dashed red and green curves, which correspond to thickness $h = 5\ell_d$, ℓ_d and $0.5\ell_d$, respectively. For the TE regime, we have three curves below the line $v = q$ marked again as 1, 2 and 3. Here, $c_s = 0.25c_T$. (Online version in colour.)

approximation of anti-plane waves in a half-space in the case of short wavelength, i.e. when the wavelength is much less than the plate thickness.

Behaviour of the dispersion curves, corresponding to the TE regime, in the neighbourhood of the wavenumber k^*, can be approximated by a linear function

$$v = \frac{c}{c_T} = 1 - A_1\xi + O(\xi^2) \quad \text{and} \quad \xi = \frac{k - k^*}{l_{dh}}. \tag{4.1}$$

Substituting (4.1) into equation (3.7) and equating coefficients at $\xi^{1/2}$, we obtain the asymptotic relations

$$k^* \approx \sqrt{\frac{1}{\bar{h}(1 - v_s^2)}} \quad \text{and} \quad A_1 = \frac{l_{dh}(1 - v_s^2)^{3/2}\bar{h}^{1/2}}{(1 + \bar{h})}, \tag{4.2}$$

where $v_s = c_{sh}/c_T$. Equation $(4.2)_1$ gives a good estimate for k^*. For example, for $v_s = 0.25$ and $h/l_{dh} = 0.1$ it gives $k^* \approx 3.266$ whereas the exact dispersion relation equation (3.7) results in $k^* = 3.265986$.

(b) Problem I. TH regime

Now we study solutions of equation (3.10) related to the TH regime. Figure 5 displays dispersion curves for $h = 0.5\ell_d$, ℓ_d and $5\ell_d$, respectively, and $c_s = 0.25c_T$. These curves lie above the horizontal line $v \equiv c/c_T = 1$. Let us note that the first curve in each series intersects the horizontal line $v = 1$ at the same point $\bar{k} = k^*$ determined by relations (4.2). These curves have a common tangent at point $(k*, 1)$ with dispersion curves of the TE regime marked also as 1, 2, 3. It seems that these curves are a continuation of the dispersion curves for the TE regime, but note that as $v = 1$ does not correspond to any wave, so this point should be excluded. Without surface enhancement we have only other dispersion curves lying above the line $v = 1$ and having limit 1 at $k \to \infty$.

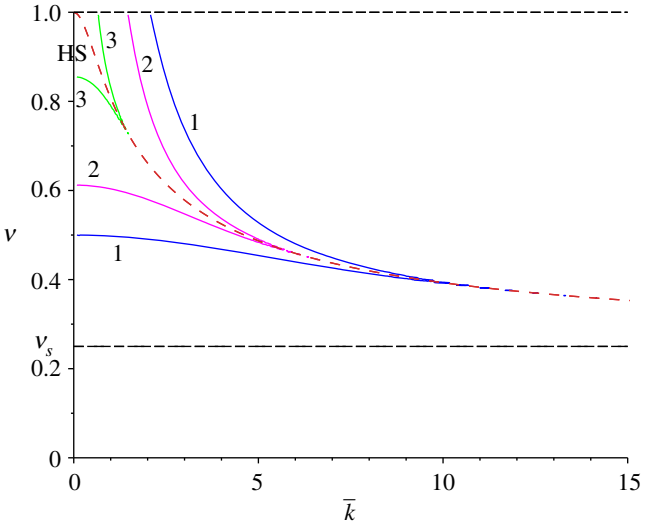

Figure 6. Problem II (TE regime), symmetric case. Dimensionless phase velocity $v = c/c_T$ versus wavenumber $\bar{k} = k\ell_d$. Curves 1, 2 and 3 correspond to thickness $h = 0.1\ell_d$, ℓ_d and $5\ell_d$, respectively. The red dashed curve marked by HS describes the case of a half-space ($h \to \infty$). Here $c_s = 0.25c_T$, $v_s = c_s/c_T$. (Online version in colour.)

(c) Problem II. TE regime

Figures 6–8 display solutions of (3.14), corresponding to the TE regime for plates with free faces, i.e for Problem II. First, in figure 6, we present dispersion curves for a symmetric in the thickness direction plate. In other words, we assume the same properties for faces, $\ell_{dh} = \ell_{d0} = \ell_d$ and $c_{sh} = c_{s0} = c_s$. Here, we see that for each $\bar{k}$, we have a couple of dispersion curves lying symmetrically below and above the HS-curve. These curves again almost coincide at $\bar{k} \to \infty$ (for short-length waves), whereas for small values of $\bar{k}$ they diverge. The curves lying above the HS-curve behave similarly to the previous case, whereas others begin with an initial value v_0 on the vertical line $\bar{k} = 0$.

For a non-symmetric case dispersion curves are given in figure 7. One can see a separation of curves related to free faces with different properties. Here, we used the value $c_{s0} = 0.5c_{sh}$, whereas $\ell_{dh} = \ell_{d0} = \ell_d$. In figure 8, $c_{s0} = 2c_{sh}$. We see that dispersion curves almost coincide with ones for half-spaces at $k \to \infty$, i.e. for short-length waves. So depending on surface properties one can expect two localized waves for a plate with two free faces.

We give also asymptotic relations for parameters v_0, k^* that are valid for both symmetric and non-symmetric cases. For curves lying under the HS-curve, the initial value of the phase velocity can be calculated by the following asymptotic relation:

$$v_0 \approx \sqrt{\frac{\bar{h} + v_{s0}^2 + v_{sh}^2}{2 + \bar{h}}} < 1. \tag{4.3}$$

Similarly to Problem I, for curves lying above the HS-curve, there is a range $\bar{k} \in (0, k^*]$ when anti-plane waves corresponding to TE regime do not exist. The asymptotic behaviour of the dispersion curves near the point k^* can be also estimated by equations (4.2). In particular, for $l_d = l_{d0} = l_{dh}$, we obtain the following approximate formula:

$$k^* \approx \sqrt{\frac{2 - v_{s0}^2 - v_{sh}^2}{\bar{h}(1 - v_{s0}^2)(1 - v_{sh}^2)}}. \tag{4.4}$$

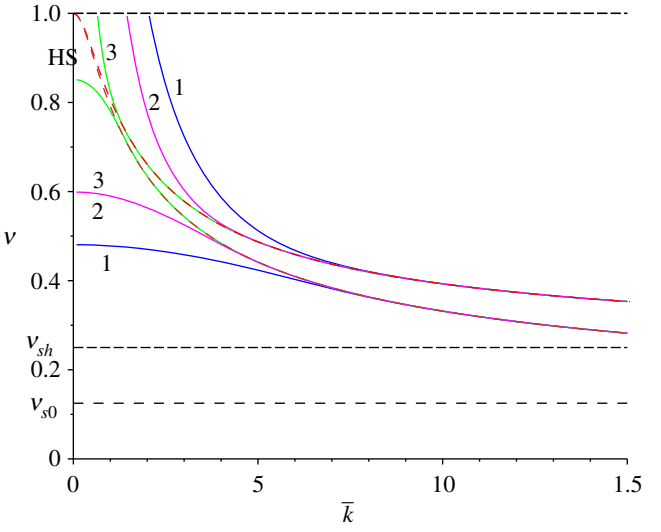

Figure 7. Problem II (TE regime), non-symmetric case. Dimensionless phase velocity $v = c/c_T$ versus wavenumber $\bar{k} = k\ell_d$. Here, $c_{sh} = 0.25c_T$ and $c_{s0} = 0.5c_{sh}$, $v_{s0} = c_{s0}/c_T$, $v_{sh} = c_{sh}/c_T$. Other data as in figure 6. (Online version in colour.)

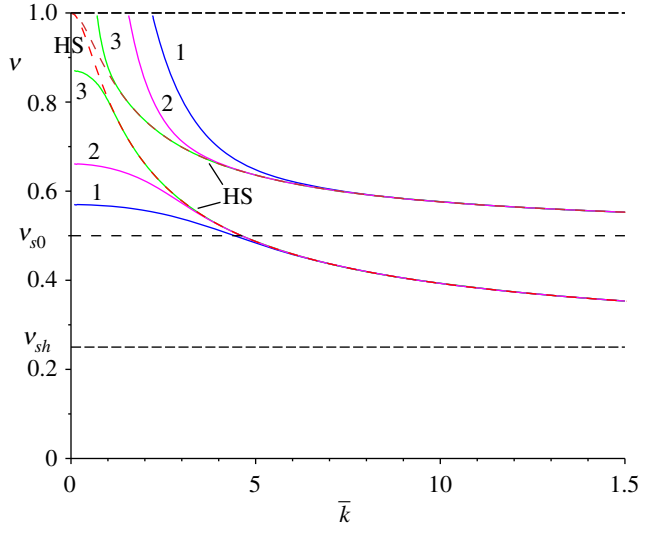

Figure 8. Problem II (TE regime), non-symmetric case. Dimensionless phase velocity $v = c/c_T$ versus wavenumber $\bar{k} = k\ell_d$. Here, $c_{sh} = 0.25c_T$ and $c_{s0} = 2c_{sh}$, $v_{s0} = c_{s0}/c_T$, $v_{sh} = c_{sh}/c_T$. Other data as in figure 7. (Online version in colour.)

(d) Problem II. TH regime

In figure 9, we present dispersion curves for a symmetric in the thickness direction plate, $\ell_{dh} = \ell_{d0} = \ell_d$ and $c_{sh} = c_{s0} = c_s$, and for $h = \ell_d$. Here, one can see blue curve 1, which begins at point $(0, 1)$, red curve 2, which intersects the horizontal line $v = 1$ at $k = k*$, and a series of green dashed curves all labelled by mark 3. Curves 1 and 2 exist only in the case of surface enhancement. Without surface stresses and inertia we have only a series of curve 3. Note that curve 1 appears in the problem with two free faces, in the case of clamped face this solution does not exist.

In figure 10, we present a rather complex picture of dispersion curves for the non-symmetric case. Here, we consider three values of the thickness, $h = 5\ell_d$, ℓ_d and $0.5\ell_d$. Corresponding

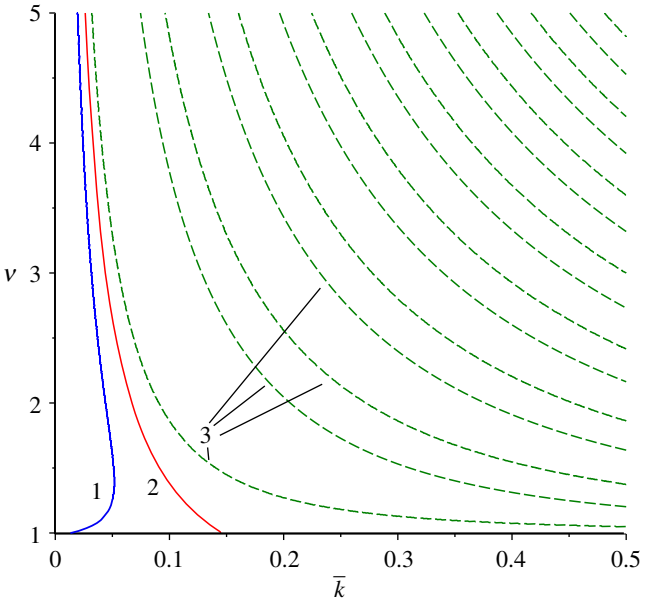

Figure 9. Problem II (TH regime), symmetric case. Dimensionless phase velocity $v = c/c_T$ versus wavenumber $\bar{k} = k\ell_d$. Here, $c_{sh} = 0.25c_T$ and $c_{s0} = c_{sh}$, $h = \ell_d$. (Online version in colour.)

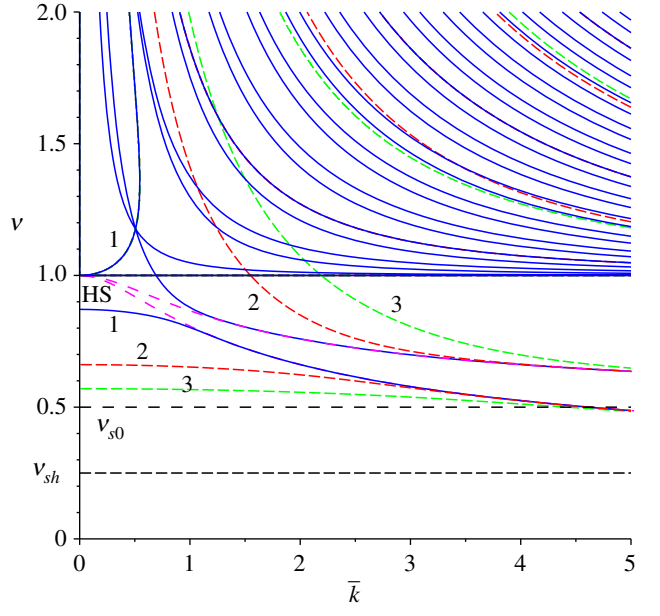

Figure 10. Problem II (TE and TH regimes), non-symmetric case. Dimensionless phase velocity $v = c/c_T$ versus wavenumber $\bar{k} = k\ell_d$. Here, $c_{sh} = 0.25c_T$ and $c_{s0} = 2c_{sh}$, $v_{s0} = c_{s0}/c_T$, $v_{sh} = c_{sh}/c_T$. Curves 1, 2 and 3 correspond to thickness $5\ell_d$, ℓ_d and $h = 0.5\ell_d$, respectively. The magenta dashed curve marked by HS describes the case of a half-space ($h \to \infty$). (Online version in colour.)

dispersion curves are marked with labels 1, 2 and 3, respectively. For larger values of h, these curves are more close to the vertical axis $k = 0$. Curves lying below line $v = 1$ are similar to ones shown in figure 8.

As in the case of Problem I, we see that the lowest dispersion curves correspond to the lowest phase speed of propagating waves and are entirely determined through the surface elastic modulus and surface mass density, i.e. determined through the surface enhancement. In other words, without surface energy we have only a harmonic regime with waves propagating with a speed higher than the transverse wave speed in the bulk.

5. Conclusion

The dispersion equations for anti-plane waves in an elastic layer (plate) have been derived for two different cases: for free-fixed faces and for free-free faces considering the linear Gurtin–Murdoch surface elasticity. The first case relates to modelling of waves propagating in a thin film perfectly attached to a rigid substrate, whereas the second one models a free suspended film or a film detached from a rigid substrate.

As in the case of elastic half-space with surface energy [32], we found a new class of waves called here exponential whose existence are determined through the presence of surface stresses and mass density. Indeed, a harmonic regime exists with or without surface enhancement, whereas an exponential regime exists only in the case of surface elasticity. Let us note that the discussed harmonic regime is similar to Lamb waves in an elastic layer [33], but not the same, as here we consider anti-plane waves. For a given wavenumber (or wavelength), we observe a series of waves propagating in an elastic layer. The waves with lowest phase speed relate to the exponential regime. The exponential regime could be interesting for experimental determination of surface properties studying the lowest speed waves in a relatively thick elastic layer or short-length waves.

For the TE regime, we conclude that the phase velocity of an anti-plane shear wave is highly sensitive to both plate thickness and boundary conditions. In particular, we have shown that

- if the wavelength is much less than the plate thickness, an anti-plane wave propagates with a velocity close to a velocity of anti-plane shear wave in a half-space;
- for a thick enough plate with free faces, we observe two anti-plane waves localized in the vicinity of faces and propagating with different speeds, in general;
- the decrease in plate thickness results in the increase in the velocity of an anti-plane shear wave;
- long-length anti-plane shear waves propagate with a velocity close to the velocity of shear wave in the bulk;
- the velocity of an anti-plane shear wave propagating along a free face with another fixed is higher that the corresponding velocity for a plate with both free faces.

The presented study may be applied to an experimental determination of surface shear moduli within the Gurtin–Murdoch surface elasticity, as was discussed in [40–42] and/or to the non-destructive evaluation of a possible delamination of thin films deposited on a rigid substrate using the difference in phase velocities.

Data accessibility. This article has no additional data.

Authors' contributions. G.I.M.: conceptualization, formal analysis, investigation, writing—original draft; M.G.B.: investigation, visualization, writing—original draft; V.A.E.: conceptualization, formal analysis, investigation, project administration, visualization, writing—original draft, writing—review and editing.

All authors gave final approval for publication and agreed to be held accountable for the work performed therein.

Conflict of interest declaration. We declare we have no competing interests.

Funding. V.A.E. acknowledges the support of the Royal Society Wolfson Visiting Fellowships program under the Project CR/212159 'Modelling of complex multiphysical phenomena on microstructured surfaces'.

References

1. Gurtin ME, Murdoch AI. 1975 A continuum theory of elastic material surfaces. *Arch. Ration. Mech. Anal.* **57**, 291–323. (doi:10.1007/BF00261375)
2. Gurtin ME, Murdoch AI. 1978 Surface stress in solids. *Int. J. Solids Struct.* **14**, 431–440. (doi:10.1016/0020-7683(78)90008-2)
3. Steigmann DJ, Ogden RW. 1997 Plane deformations of elastic solids with intrinsic boundary elasticity. *Proc. R. Soc. A* **453**, 853–877. (doi:10.1098/rspa.1997.0047)
4. Steigmann DJ, Ogden RW. 1999 Elastic surface-substrate interactions. *Proc. R. Soc. A* **455**, 437–474. (doi:10.1098/rspa.1999.0320)
5. Huang ZP, Wang JX. 2006 A theory of hyperelasticity of multi-phase media with surface/interface energy effect. *Acta Mech.* **182**, 195–210. (doi:10.1007/s00707-005-0286-3)
6. Duan HL, Wang J, Karihaloo BL. 2008 Theory of elasticity at the nanoscale. *Adv. Appl. Mech.* **42**, 1–68. (doi:10.1016/S0065-2156(08)00001-X)
7. Ru CQ. 2010 Simple geometrical explanation of Gurtin-Murdoch model of surface elasticity with clarification of its related versions. *Sci. China Phys., Mech. Astron.* **53**, 536–544. (doi:10.1007/s11433-010-0144-8)
8. Wang J, Huang Z, Duan H, Yu S, Feng X, Wang G, Zhang W, Wang T. 2011 Surface stress effect in mechanics of nanostructured materials. *Acta Mech. Solida Sin.* **24**, 52–82. (doi:10.1016/S0894-9166(11)60009-8)
9. Javili A, McBride A, Steinmann P. 2013 Thermomechanics of solids with lower-dimensional energetics: on the importance of surface, interface, and curve structures at the nanoscale. A unifying review. *Appl. Mech. Rev.* **65**, 010802. (doi:10.1115/1.4023012)
10. Eremeyev VA. 2016 On effective properties of materials at the nano- and microscales considering surface effects. *Acta Mech.* **227**, 29–42. (doi:10.1007/s00707-015-1427-y)
11. Benveniste Y, Miloh T. 2001 Imperfect soft and stiff interfaces in two-dimensional elasticity. *Mech. Mater.* **33**, 309–323. (doi:10.1016/S0167-6636(01)00055-2)
12. Benveniste Y, Miloh T. 2007 Soft neutral elastic inhomogeneities with membrane-type interface conditions. *J. Elast.* **88**, 87–111. (doi:10.1007/s10659-007-9115-3)
13. Mishuris GS, Movchan NV, Movchan AB. 2006 Steady-state motion of a mode-III crack on imperfect interfaces. *Q. J. Mech. Appl. Math.* **59**, 487–516. (doi:10.1093/qjmam/hbl013)
14. Mishuris G, Öchsner A, Kuhn G. 2006 FEM-analysis of nonclassical transmission conditions between elastic structures. Part 2: stiff imperfect interface. *CMC: Comput., Mater. Continua* **4**, 137–152.
15. Mishuris GS, Movchan NV, Movchan AB. 2010 Dynamic mode-III interface crack in a bi-material strip. *Int. J. Fract.* **166**, 121–133. (doi:10.1007/s10704-010-9507-4)
16. Berdichevsky VL. 2010 Nonlinear theory of hard-skin plates and shells. *Int. J. Eng. Sci.* **48**, 357–369. (doi:10.1016/j.ijengsci.2009.09.003)
17. Eremeyev VA, Rosi G, Naili S. 2020 Transverse surface waves on a cylindrical surface with coating. *Int. J. Eng. Sci.* **147**, 103188. (doi:10.1016/j.ijengsci.2019.103188)
18. Gorbushin N, Eremeyev VA, Mishuris G. 2020 On stress singularity near the tip of a crack with surface stresses. *Int. J. Eng. Sci.* **146**, 103183. (doi:10.1016/j.ijengsci.2019.103183)
19. Kaplunov J, Prikazchikov DA. 2017 Asymptotic theory for Rayleigh and Rayleigh-type waves. *Adv. Appl. Mech.* **50**, 1–106. (doi:10.1016/bs.aams.2017.01.001)
20. Chebakov R, Kaplunov J, Rogerson GA. 2016 Refined boundary conditions on the free surface of an elastic half-space taking into account non-local effects. *Proc. R. Soc. A* **472**, 20150800.
21. Mishuris GS, Movchan AB, Slepyan LI. 2009 Localised knife waves in a structured interface. *J. Mech. Phys. Solids* **57**, 1958–1979. (doi:10.1016/j.jmps.2009.08.004)
22. Gorbushin N, Mishuris G. 2016 Dynamic crack propagation along the interface with non-local interactions. *J. Eur. Ceram. Soc.* **36**, 2241–2244. (doi:10.1016/j.jeurceramsoc.2015.12.048)
23. Li L, Lin R, Ng TY. 2020 Contribution of nonlocality to surface elasticity. *Int. J. Eng. Sci.* **152**, 103311. (doi:10.1016/j.ijengsci.2020.103311)
24. Kaplunov J, Prikazchikov D, Sultanova L. 2019 Rayleigh-type waves on a coated elastic half-space with a clamped surface. *Phil. Trans. R. Soc. A* **377**, 20190111. (doi:10.1098/rsta.2019.0111)
25. Mindlin RD. 1965 Second gradient of strain and surface-tension in linear elasticity. *Int. J. Solids Struct.* **1**, 417–438. (doi:10.1016/0020-7683(65)90006-5)
26. Eremeyev VA, Rosi G, Naili S. 2019 Comparison of anti-plane surface waves in strain-gradient materials and materials with surface stresses. *Math. Mech. Solids* **24**, 2526–2535. (doi:10.1177/1081286518769960)

27. Korteweg DJ. 1901 Sur la forme que prennent les équations des mouvements des fluides si l'on tient compte des forces capillaires par des variations de densité. *Archives Néerlandaises des sciences exactes et naturelles* **Sér. II**, 1–24.
28. Eremeyev VA, Sharma BL. 2019 Anti-plane surface waves in media with surface structure: Discrete vs. continuum model. *Int. J. Eng. Sci.* **143**, 33–38. (doi:10.1016/j.ijengsci.2019.06.007)
29. Mogilevskaya SG, Zemlyanova AY, Kushch VI. 2021 Fiber-and particle-reinforced composite materials with the Gurtin–Murdoch and Steigmann–Ogden surface energy endowed interfaces. *Appl. Mech. Rev.* **73**, 1–18. (doi:10.1115/1.4051880)
30. Mogilevskaya SG, Zemlyanova AY, Mantič V. 2021 The use of the Gurtin–Murdoch theory for modeling mechanical processes in composites with two–dimensional reinforcements. *Compos. Sci. Technol.* **210**, 108751. (doi:10.1016/j.compscitech.2021.108751)
31. Kim CI, Ru CQ, Schiavone P. 2013 A clarification of the role of crack-tip conditions in linear elasticity with surface effects. *Math. Mech. Solids* **18**, 59–66. (doi:10.1177/1081286511435227)
32. Eremeyev VA, Rosi G, Naili S. 2016 Surface/interfacial anti-plane waves in solids with surface energy. *Mech. Res. Commun.* **74**, 8–13. (doi:10.1016/j.mechrescom.2016.02.018)
33. Achenbach J. 1973 *Wave Propagation in Elastic Solids*. Amsterdam, The Netherland: North Holland.
34. Chen WQ, Wu B, Zhang CL, Zhang C. 2014 On wave propagation in anisotropic elastic cylinders at nanoscale: surface elasticity and its effect. *Acta Mech.* **225**, 2743–2760. (doi:10.1007/s00707-014-1211-4)
35. Eremeyev VA. 2020 Strongly anisotropic surface elasticity and antiplane surface waves. *Phil. Trans. R. Soc. A* **378**, 20190100. (doi:10.1098/rsta.2019.0100)
36. Xu L, Fan H. 2016 Torsional waves in nanowires with surface elasticity effect. *Acta Mech.* **227**, 1783–1790. (doi:10.1007/s00707-016-1607-4)
37. Huang Z. 2018 Torsional wave and vibration subjected to constraint of surface elasticity. *Acta Mech.* **229**, 1171–1182. (doi:10.1007/s00707-017-2047-5)
38. Zhu F, Pan E, Qian Z, Wang Y. 2019 Dispersion curves, mode shapes, stresses and energies of SH and Lamb waves in layered elastic nanoplates with surface/interface effect. *Int. J. Eng. Sci.* **142**, 170–184. (doi:10.1016/j.ijengsci.2019.06.003)
39. Mikhasev GI, Botogova MG, Eremeyev VA. 2021 On the influence of a surface roughness on propagation of anti-plane short-length localized waves in a medium with surface coating. *Int. J. Eng. Sci.* **158**, 103428. (doi:10.1016/j.ijengsci.2020.103428)
40. Jia F, Zhang Z, Zhang H, Feng XQ, Gu B. 2018 Shear horizontal wave dispersion in nanolayers with surface effects and determination of surface elastic constants. *Thin Solid Films* **645**, 134–138. (doi:10.1016/j.tsf.2017.10.025)
41. Wu W, Zhang H, Jia F, Yang X, Liu H, Yuan W, Feng XQ, Gu B. 2020 Surface effects on frequency dispersion characteristics of Lamb waves in a nanoplate. *Thin Solid Films* **697**, 137831. (doi:10.1016/j.tsf.2020.137831)
42. Jia N, Peng Z, Li J, Yao Y, Chen S. 2021 Dispersive behavior of high frequency Rayleigh waves propagating on an elastic half space. *Acta Mech. Sin.* **37**, 562–569. (doi:10.1007/s10409-020-01009-3)
43. Grekov MA, Kostyrko SA. 2016 Surface effects in an elastic solid with nanosized surface asperities. *Int. J. Solids Struct.* **96**, 153–161. (doi:10.1016/j.ijsolstr.2016.06.013)
44. Kostyrko S, Grekov M, Altenbach H. 2019 Stress concentration analysis of nanosized thin-film coating with rough interface. *Contin. Mech. Thermodyn.* **31**, 1863–1871. (doi:10.1007/s00161-019-00780-4)